UDK 621.762:669.245:669.794
Original scientific article/Izvirni znanstveni članek

ISSN 1580-2949
MTAEC9, 48(6)899(2014)

EVALUATION OF THE MECHANICAL PROPERTIES OF A HOT ISOSTATICALLY PRESSED YTTRIA-DISPERSED NICKEL-BASED SUPERALLOY

VREDNOTENJE MEHANSKIH LASTNOSTI Ni-SUPERZLITINE Z DISPERGIRANIM ITRIJEM PO VROČEM IZOSTATSKEM STISKANJU

Monika Mohan[1], Ramanathan Subramanian[1], Md. Zafir Alam[2], Peter Chrysologue Angelo[1]

[1]Department of Metallurgical Engineering, PSG College of Technology, Peelamedu, Coimbatore 641 004, Tamil Nadu, India
[2]Defence Metallurgical Research Laboratory, Defence Research and Development Organization, Ministry of Defence, Government of India, Kanchanbagh (PO), Hyderabad 500 058, India
moni_london@yahoo.co.in

Prejem rokopisa – received: 2013-11-28; sprejem za objavo – accepted for publication: 2013-12-12

Nickel-based oxide-dispersion-strengthened superalloys, reinforced with yttria, are used as high-temperature materials owing to their superior creep strength, fatigue strength, excellent oxidation and hot corrosion resistance. Nanosized yttria particles help to inhibit the grain growth and act as obstacles against dislocation motion. In the present work elemental powders were milled along with yttria (w = 0.6 %) and the effects of the milling time and milling speed on the alloy behavior were studied using XRD, SEM/EDS and TEM. The alloying elements formed a solid solution after 40 h of milling at 300 r/min, achieving the nanocrystallite size (18 nm). The TEM analysis confirmed the formation of nanocrystalline face-centered cubic Ni-solid solution and severe plastic deformation occurring during mechanical alloying was confirmed with the formation of Moiré fringes. The consolidation of the powders with the hot-isostatic-pressing (HIP) technique gave a microhardness value of 4.2 GPa. The TEM analysis of a HIPed sample revealed a solutionized phase with the mean grain size of 196 nm. The modulus of elasticity, *YS* and *UTS* evaluated with a micro-tensile test at a strain rate of 10^{-3} s^{-1} gave the values, at RT, of 177 GPa, 958 MPa and 958 MPa, respectively, and at 1200 °C the values were 109 GPa, 39 MPa and 59 MPa, respectively.

Keywords: ODS alloys, nickel, yttria, mechanical alloying, HIP, micro-tensile test

Superzlitine na osnovi niklja, ojačane z delci itrijevega oksida, se uporabljajo kot visokotemperaturni material zaradi svoje velike odpornosti proti lezenju, odpornosti proti utrujanju ter odlične odpornosti proti visokotemperaturni oksidaciji in koroziji. Itrijevi delci nanovelikosti pomagajo pri preprečevanju rasti zrn in delujejo kot ovira pri gibanju dislokacij. V predstavljenem delu so bile mlete mešanice elementni prahovi z itrijem (w = 0,6 %), z XRD, SEM/EDS in TEM pa je bil preiskovan vpliv trajanja in hitrosti mletja na lastnosti zlitine. Legirni elementi so tvorili po 40 h mletja pri 300 r/min trdno raztopino z nanokristaliti velikosti 18 nm. Analiza s TEM je potrdila nastanek nanokristalinične trdne raztopine Ni s ploskovno centrirano kubično rešetko in močno plastično deformacijo med mehanskim legiranjem, ki je bila potrjena z nastankom Moirovih obročev. Po zgoščevanju prahov s tehniko vročega izostatskega stiskanja (HIP) je bila mikrotrdota materiala 4,2 GPa. TEM-analiza vzorcev po HIP je odkrila homogene faze s povprečno velikostjo zrn 196 nm. Pri sobni temperaturi je bil določen modul elastičnosti 177 GPa, meja plastičnosti (*YS*) 958 MPa in natezna trdnost (*UTS*) 958 MPa ter 109 GPa, 39 MPa in 59 MPa pri temperaturi 1200 °C.

Ključne besede: ODS-zlitine, nikelj, itrij, mehansko legiranje, HIP, mikro natezni preizkus

1 INTRODUCTION

With the onset of the gas-turbine technology, nickel-based alloys started to replace Fe-based alloys since they exhibit better creep and fatigue properties due to the presence of ordered (γ') precipitates.[1] However, these precipitates coarsen at high temperatures, leading to a loss of strength. Cast and wrought superalloys had problems pertaining to grain coarsening and chemical inhomogeneity arising from segregation as well as the presence of oxides and carbonitrides. In the early 1970s the powder-metallurgy (P/M) route for the production of these alloys gained momentum.[2] The P/M technique offers advantages over conventional techniques for the production of superalloys suitable for high-temperature applications through stringent quality control as well as through elimination of non-metallic inclusions and other contaminants using inert gas processing.[3] Benjamin and co-workers[4] initiated the work on oxide-dispersion-strengthened (ODS) alloys using the mechanical-alloying route at Paul D. Merica Research Laboratory of the International Nickel Company (INCO). Oxide-dispersion-strengthened nickel-based alloys were developed as potential candidate materials for aircraft gas turbines including the combustor, transition pieces, turbine vanes, blades and disks.[5] ODS alloys have been efficiently synthesized through mechanical alloying (MA)[6,7] by uniformly dispersing yttria in a suitable matrix by mixing elemental/pre-alloyed powders followed by hot isostatic pressing (HIP) or hot extrusion. Nanosized yttria contributes to the creep strength through a dislocation/dispersion interaction in Fe- and Ni-ODS alloys and enhances work hardening during MA, thereby accelerating alloy formation.[8–10]

The present work involves a consolidation of an yttria-dispersion-strengthened Ni-based alloy with the hot-isostatic-pressing technique and an evaluation of high-temperature tensile properties using a small-dimension specimen. An attempt was made to synthesize Ni-ODS powders with mechanical alloying (MA) and a subsequent consolidation using HIP to get ultrafine grains. The study also investigates the influence of the milling times and milling speed on the particle size and microstructure of the alloy powders and microstructural evolution after the consolidation. A detailed powder characterization was carried out to optimize the process parameters using XRD, SEM/EDS, TEM and X-ray elemental mapping. A micro-tensile test was used to evaluate the high-temperature as well as room-temperature mechanical properties. An attempt was made to study the tensile behavior using the specimens only a few micrometers thick. The challenge was to fabricate these samples by electro-discharge machining (EDM) and then gripping the samples against the walls of the slots, confirming the failure to occur within the gauge length and study the type of fracture.

2 EXPERIMENTAL METHODOLGY

Appropriate quantities of high-purity (99 %) elemental powders were ball milled so as to have the final chemical mass composition (*w*/%) of 20Cr-3Fe-0.5Ti-0.3Al-0.6Y_2O_3-Bal.Ni using stearic acid (a process-control agent) in a Retsch PM 400 planetary ball mill. High-chrome steel balls of a diameter 10 mm were chosen as the milling media with a ball-to-powder (BPR) mass ratio of 10 : 1. The powder morphology and size distribution of the particles were investigated using a JEOL scanning electron microscope (model JSM-6360) operating at 20 kV. A bulk X-ray diffraction analysis (XRD) was done using Co K_α radiation (λ = 0.1789 nm) with a Shimadzu XRD-6000 operating at 30 kV/30 mA with a scanning speed of 1°/min. Mechanically alloyed powders were dispersed in ethanol, sonicated for 15 min and placed on a copper grid for a TEM analysis. Structural details of the alloy powders were determined using a JEOL JEM-2100 HRTEM operating at 200 kV. The powders were compacted with hot isostatic pressing (Engineered Pressure Systems, Belgium, Model EPSI-HIP) after filling the milled powders into the SS capsules with a diameter 38 mm, thickness 1.5 mm and height 90 mm. The powder-filled capsules were evacuated at room temperature to a vacuum level of $6.6 \cdot 10^{-4}$ mbar and subsequently hot degassed at 773 K for about 5 h and crimp sealed under a dynamic vacuum level of $6.6 \cdot 10^{-6}$ mbar. HIPing was carried out at a temperature of 1453 K under a pressure 1200 bar for a dwell time of 3 h. The heating and cooling rates of HIPing were about 283 K/min. The sintered sample was cooled down to room temperature. The microhardness of the polished surface was measured using a Mitutoyo microhardness tester at a load of 500 g for 20 s. Small circular samples were EDM wire cut from the HIPed alloy. Micro-tensile samples were machined and thinned down by careful polishing using 600, 1000, 1200 and 2000 grit polishing papers and the final polishing was done with a diamond paste 0.5 µm. The samples were reduced to the final thickness of 200 µm over its entire area. The samples were fastened using slotted grips in order to ensure that the samples would not move while performing the tensile test. The samples were heated with the resistance-heating method employing the DC current. The temperature was

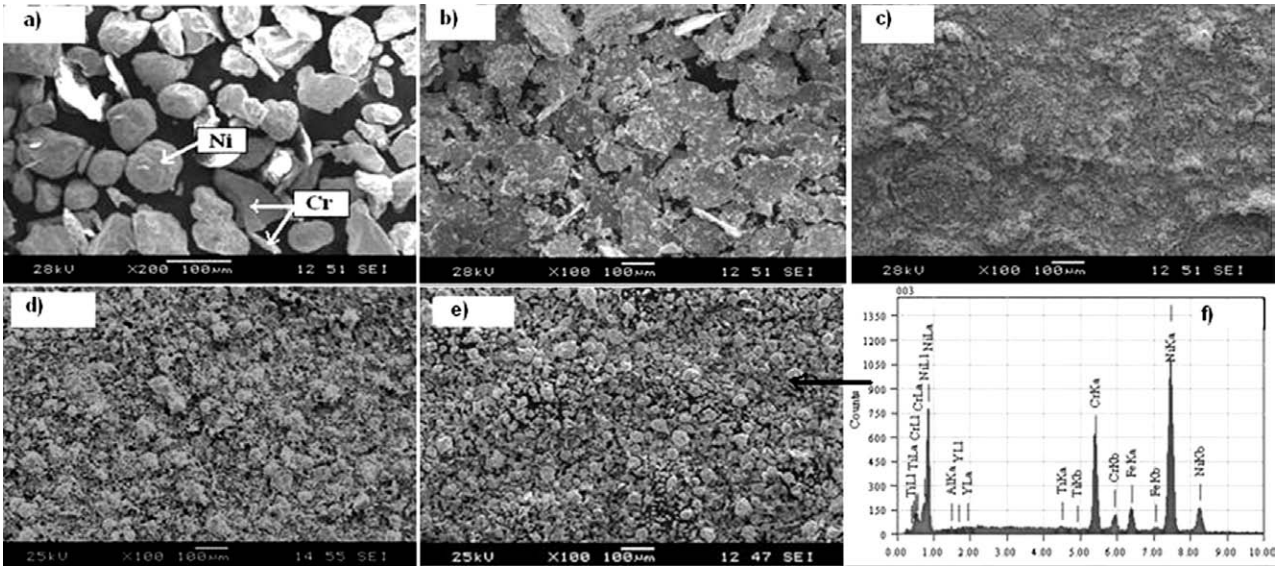

Figure 1: SEM micrographs of: a) the as-mixed state and ODS powders milled for: b) 5 h, c) 20 h, d) 30 h, e) 40 h and f) EDAX analysis of MA powders after 40 h

Slika 1: SEM-posnetki: a) po mešanju in ODS prahovi mleti po: b) 5 h, c) 20 h, d) 30 h, e) 40 h in f) EDAX-analiza mehansko legiranih (MA) prahov po 40 h

maintained within the gauge-length region because of the small cross-section. A smaller area generates high electrical resistance, thereby heating the gauge-length portion while the remaining portions were at lower temperatures. A Walterbai Ag (Switzerland) micro-tensile testing machine was used to test the miniature samples using a load 5000 N at a strain rate of 10^{-3} s^{-1}. To measure the strain in a specimen during the test, an optical video extensometer with a resolution of 10 microstrain was used. The stress-strain plot was recorded in a computer attached to the machine. Three samples were tested for each condition to check the reproducibility.

3 RESULTS AND DISCUSSION

3.1 SEM and particle-size analysis

A SEM micrograph (**Figure 1a**) shows the shapes and distribution of elemental-powder particles in the as-mixed state. Nickel powders show a rounded shape, while chromium powders show an irregular shape. The SEM analysis of the ODS powder samples milled at 300 r/min showed various stages of MA (**Figures 1b** to **1e**). The flattening, deformation and cold welding of powder particles resulted in a subsequent breakup of the particles. The energy-dispersive-spectroscopy (EDS) analysis was carried out for the powders milled for 40 h (**Figure 1f**). The compositional analysis showed the presence of the constituent elements along with yttria. The spot analysis indicated a complete alloying with no contamination, indicating the purity of the alloyed powders.

3.2 XRD investigation

XRD patterns of the powders ball milled at 300 r/min (**Figure 2**) show only Ni and Cr peaks. A continuous decrease in the intensity of the Ni(111) peaks was observed with an increase in the milling time. A gradual

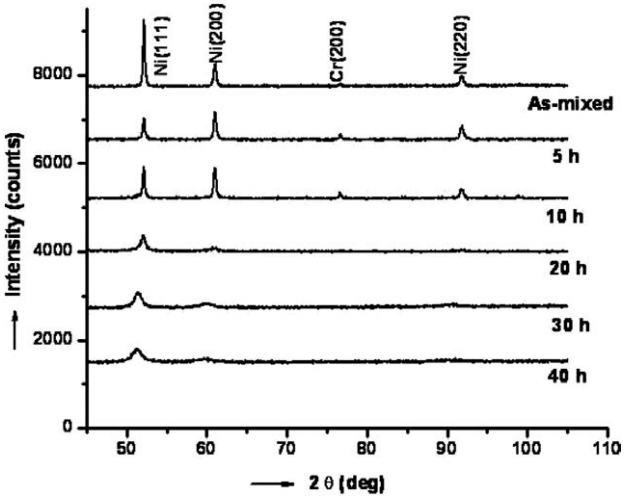

Figure 2: XRD of the powders ball milled at 300 r/min
Slika 2: XRD-posnetki prahov, mletih s kroglami pri 300 r/min

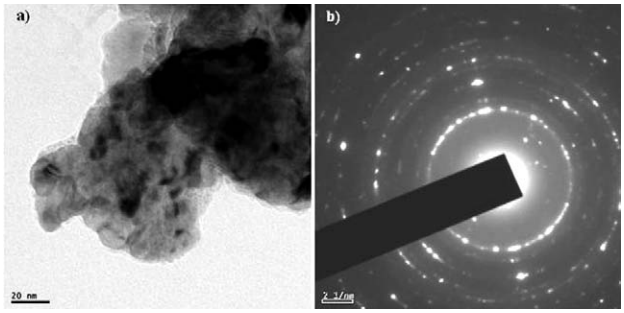

Figure 3: a) Bright-field HR image showing intense deformation and b) SAED pattern of the powders milled for 20 h at 300 r/min
Slika 3: a) HR-posnetek s svetlim ozadjem prikazuje močne deformacije in b) SAED-vzorec prahov, mletih 20 h pri 300 r/min

peak broadening due to the accumulation of strain in the powders was observed although in a broader aspect all of the reduced crystallite sizes, lattice strains and instrumental effects add to the broadening of the peaks in XRD.[11] In order to correct the instrumental broadening effects, standard nickel powder was selected. The crystallite size and lattice strain of the milled powders were calculated using a pseudo-Voigt function.[12] After 40 h complete dissolution of the Cr(200), Ni(200) and Ni(220) peaks and a shift of the Ni(111) peak to lower Bragg angles proved the completion of the solid solution. A significant reduction in the crystallite size was observed between 10 h and 20 h of milling but after 40 h no grain refinement occurred. The powders milled at 300 r/min attained a crystallite size of 18 nm after a milling time of 40 h. Zhang et al.[13] showed that MA of the Co-based ODS alloys showed high hardness up to 15 h and after that the hardness remained constant reaching the minimum size of 50 nm.

3.3 TEM studies

To study the changes evolved in the microstructures at different milling times for the powders ball milled at 300 r/min, the powders were investigated with a high-resolution transmission electron microscope (HRTEM). The TEM microstructures of the powders milled for 20 h at 300 r/min showed typical features of the mechanically

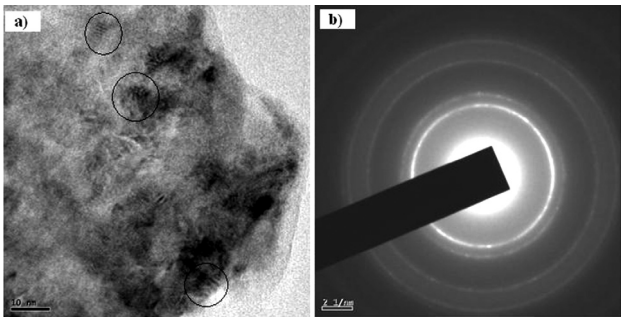

Figure 4: a) Powders ball milled for 30 h at 300 r/min showing Moiré fringes and b) SAED pattern
Slika 4: a) Prahovi, mleti s kroglami 30 h pri 300 r/min prikazujejo Moirove obroče in b) SAED-vzorec

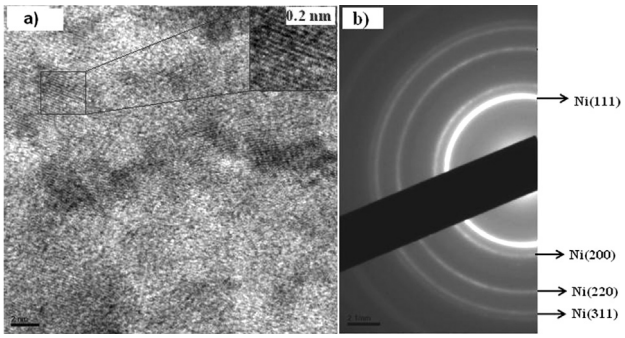

Figure 5: a) HRTEM image showing an enlarged portion of {111} lattice fringe, b) SAED pattern showing continuous rings after ball milling for 40 h at 300 r/min

Slika 5: a) HRTEM-posnetek prikazuje povečan delež {111} mrežnih obročev, b) SAED vzorec, ki prikazuje zvezne kroge po mletju s kroglami 40 h pri 300 r/min

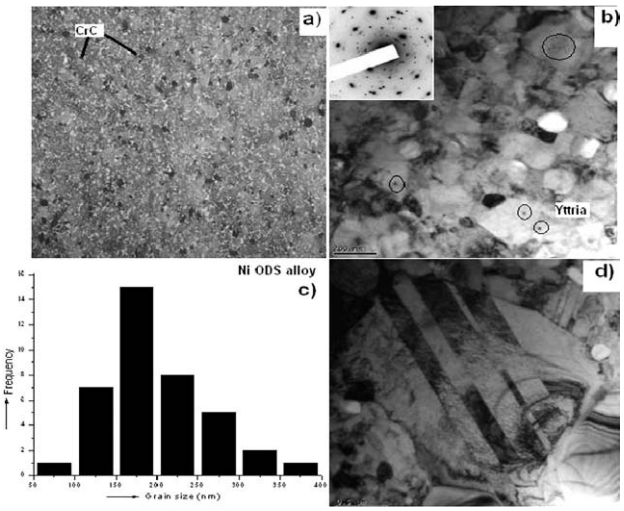

Figure 6: a) Light micrograph of a HIPed sample showing chromium carbide precipitates, b) bright-field image after HIP at 1453 K (SAD pattern in the inset) showing ultrafine grains and nanosized yttria (in the circles), c) grain size distribution of the HIP sample and d) micrograph showing the presence of annealing twins

Slika 6: a) Svetlobni posnetek vzorca po HIP prikazuje izločke kromovega karbida, b) posnetek s svetlim ozadjem po HIP pri 1453 K s SAD-vzorcem, ki prikazuje ultra drobna zrna itrija (v krogcih), c) razporeditev velikosti zrn vzorca po HIP in d) mikroposnetek, ki prikazuje prisotnost transformacijskih dvojčkov

alloyed powder particles. The bright-field image (**Figure 3a**) and the presence of a spotty ring pattern of SAD (selected area diffraction) (**Figure 3b**) provided the evidence for nanograins. A TEM image taken after 30 h (**Figure 4a**) revealed the presence of Moiré fringes which arose due to numerous nanosized grains stacked in the bulk sample. Hence, it can be inferred that a significant size reduction of the grains occurred during the milling 30 h. The change in the SAD pattern from discontinuous rings to a set of continuous rings (**Figure 4b**) and the appearance of continuous rings proved the presence of nanograin particles. This can be explained with the fact that for a smaller crystallite size the rings of SAD are more continuous and for a larger crystallite size the rings appear as spots.[14] A similar pattern was observed in MA Ni-Cr [15] due to a refinement of the crystallite size. Moiré fringes were reported for the MA NiAl powders milled for 24 h [16] and Fe_3Al intermetallic nanopowders with the spacing between 10–20 nm.[17] A HRTEM image of a sample milled for 40 h (**Figure 5a**) was analyzed and the distance between the lattice fringes was calculated to be 0.20 nm corresponding to the {111} lattice fringe of nickel. The continuous rings observed in the SAD pattern (**Figure 5b**) also confirm the presence of nanocrystallites. The rings were indexed, showing the most intense peaks, namely, Ni(111), Ni(200), Ni(220) and Ni(311). The absence of the solute Cr rings confirmed the formation of a single-phase FCC Ni-solid solution.

3.4 Microstructural analysis of hot isostatically pressed samples

The etched microstructure (using Kalling's reagent) of the HIPed compact (**Figure 6a**) showed a solutionized phase and sparingly distributed dark-colored chromium-carbide precipitates (as determined with the EDAX point analysis). HIP enhances the effect of the MC carbides that appear within the grain boundaries and are helpful in improving the stress-rupture life by preventing grain-boundary sliding.[18] The same was observed, as bright particles in the as-hot-isostatically-pressed alloy of Inconel 718, by Appa Rao et al.[19] **Figure 6b** shows a TEM image of the powders ball milled for 40 h and hot isostatically pressed at 1453 K. The bright-field image and the spotty rings in the SAD pattern show ultrafine grains in the consolidated sample and the presence of only the Ni phase. Spherical yttria dispersions with a size of 20 nm are homogeneously embedded in the Ni matrix. The size of the nano-yttria particles remained the same indicating no further coarsening, even after being subjected to a high consolidating temperature. The grain-size distribution determined from the TEM images showed that the mean grain size of the hot isostatically pressed sample was 196 nm (**Figure 6c**). The microhardness value, taken as the average of 10 indentations on the HIPed sample was 4.2 GPa. A few annealing twins (**Figure 6d**) were also observed which could probably be due to high temperature consolidation. In some areas the twins were broader and in other areas they appeared to be narrower. Twins have a tendency of increasing the strength of the material as they obstruct the dislocation motion. However, the overall strength contributed by twining is lower than the strength contributed by pinning up the grain boundaries with yttria dispersions.

3.5 Tensile-property evaluation of hot isostatically pressed samples

To investigate the mechanical properties, micro-tensile specimens were EDM wire cut from the HIPed sample. The main advantages of a micro-tensile test are a

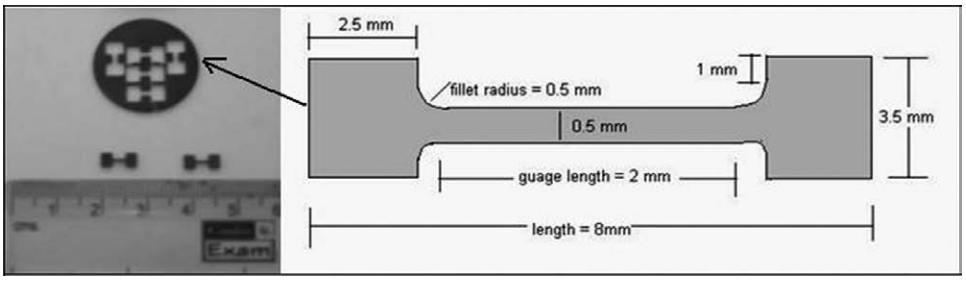

Figure 7: Schematic diagram showing a micro-tensile specimen, EDM wire cut from the HIPed sample
Slika 7: Shematski prikaz mikro nateznega vzorca, izrezanega z žično erozijo (EDM) iz vroče izostatsko stisnjenega (HIP) vzorca

uniform strain generated in a specimen during the test compared to the other indentation techniques, the interpretation that is also much simpler and the mechanical response generated that is representative of the alloy. The tensile-test specifications were selected on the basis of the work done by Alam et al.[20] It was ensured that the samples followed the HL rule of *R* being equal to 2 and that the breakage occurred within the gauge length. A schematic diagram shows a micro-tensile test specimen exhibiting a well-defined gauge section with the cross-sectional dimension, the thicknesses of a few micrometers (**Figure 7**). The tensile properties of the HIPed alloy tested at room temperature and elevated temperatures are shown in **Table 1**. The values were compared with the data for the Schwarzkopf Plansee PM1000 alloy in a spreadsheet form. The yield strength, ultimate tensile strength and modulus of elasticity at room temperature for the PM1000 alloy (a textured sample) were reported[21] to be 626 MPa, 95 MPa and 150 GPa, respectively, while the values for the synthesized alloy were much higher, 958 MPa, 958 MPa and 177 GPa, respectively. The yield and ultimate-tensile-strength values were almost in alignment with the PM1000 alloy but a slight deviation took place with the increase in the temperature. As the temperature increased, the elastic modulus, yield strength and ultimate tensile strength decreased; in contrast, the alloy showed some ductility at elevated temperatures. The observations from the stress-strain diagram (**Figure 8**) showed that there was not any appreciable plasticity of the specimens tested up to 900 °C, i.e., the variation in the ductility, as presented by the plastic-strain-to-fracture at 900 °C. Beyond this temperature the alloy exhibited a noticeable change in the ductility and the samples also broke in a ductile fashion. A clear brittle-to-ductile transition (BDTT) was observed at 1000 °C, quite high for nickel-based superalloys. The lack of appreciable plastic strain indicated that the alloy was inherently brittle. The reason for the inherent brittleness of the alloy could be the non-fulfillment of the Von Mises criterion, namely, the minimum of five slip systems for the ductility in polycrystalline materials, although some plastic deformation may be obtained if there is twinning or some preferred orientation. Moreover, the presence of second-phase particles in the continuous-matrix phase

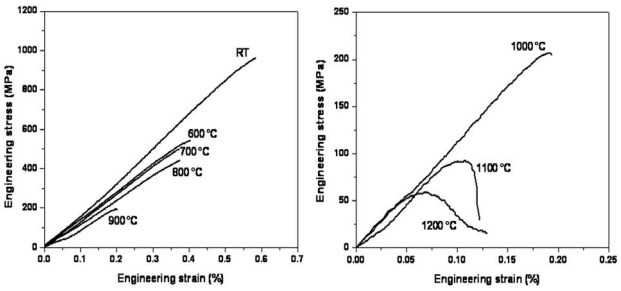

Figure 8: Stress-strain graphs of the samples tested at various temperatures
Slika 8: Prikaz krivulj napetost – raztezek za vzorce, preizkušene pri različnih temperaturah

Table 1: Variation in the mechanical properties with respect to temperature
Tabela 1: Spreminjanje mehanskih lastnosti glede na temperaturo

Test temperature	*E*/(GPa)	*YS*/(MPa)/ *FS*/(MPa)	*UTS*/(MPa)	Plastic strain (%)
RT	177	958	958	0.013
600 °C	139	532	532	0.013
700 °C	137	497	497	0.014
800 °C	123	436	436	0.021
900 °C	121	193	193	0.043
1000 °C	115	189	207	0.014
1100 °C	120	75	92	0.117
1200 °C	109	39	59	0.120

results in localized internal stresses which could modify the plastic properties of the continuous phase. Such low plastic yielding at elevated temperatures was also reported by Alam et al.[20] for coated materials. The as-HIPed alloy tended to give lower ductility and stress-rupture properties due to prior particle boundaries (PPBs); however, further thermo-mechanical treatments[19,22] can improve the strength and ductility by eliminating PPBs as reported by Appa Rao et al.[19] Extrusion after HIP causes enhanced strength and ductility of powder-metallurgy Mo- and Nb-silicide alloys and it is also known to reduce BDTT by 200 °C.[22] Another reason for the loss in ductility could be due to artifacts (like porosity and microcracks) and artifact-free samples are difficult to achieve.[23] The samples tested at (1000, 1100 and 1200) °C showed an increased elongation due to the strain-hardening effect, a process called dislocation accumulation which occurs before failure.[23]

Ductility can be enhanced in the case of larger grains as larger amounts of slip can occur; however, in fine-sized grains slip is restricted and the fracture tends to become more brittle. The presence of Cr-rich precipitates and the change in morphology at elevated temperatures could also affect the BDTT.[24]

4 CONCLUSIONS

1. The elemental-powder mix led to the formation of a Ni solid solution after being milled for 40 h at the optimized milling speed of 300 r/min, having a crystallite size of 18 nm.
2. Energy-dispersive-spectroscopy studies confirmed the purity of the alloy powder.
3. The presence of Moiré fringes and continuous rings in the SAD pattern and dark-field images confirmed the formation of nanograins in the Ni-ODS alloy. The lattice fringes were found to be 0.20 nm apart, corresponding to the FCC Ni-phase.
4. The powders milled for 40 h and consolidated with HIP had the mean grain size of 196 nm and a microhardness of 4.2 GPa.
5. When using smaller-dimension samples, TEM images revealed a uniform distribution of nanosized yttria particles, thereby showing *YS*, *UTS* and the elastic modulus to be 958 MPa, 958 MPa and 177 GPa, respectively, at room temperature and a strain rate of 10^{-3} s^{-1}.
6. *YS* and *UTS* were found to decrease with an increase in the temperature with some marginal ductility beyond 1000 °C, showing a clear brittle-to-ductile transition.

Acknowledgements

One of the authors (Monika Mohan) gratefully acknowledges DST, New Delhi, for financial support (SR/WOS-A/ET-09/2009) under the Women Scientists Scheme (WOS-A). Thanks are due to Dr. G. Appa Rao, Defence Metallurgical Research Laboratory (DMRL), Defence Research and Development Organization (DRDO), Ministry of Defence, for helping us with the HIP compaction, and to the Principal, PSG College of Technology, for providing the facilities.

5 REFERENCES

[1] J. Lacaze, A. Hazotte, Directionally solidified materials: Ni-base superalloys for gas turbines, Textures and Microstructures, 13 (**1990**) 1, 1–14

[2] D. Furrer, H. Fecht, Nickel-based superalloys for turbine discs, JOM, 51 (**1999**) 1, 14–17

[3] N. S. Babu, S. B. Tiwari, B. N. Rao, Development and validation of processing maps for nickel based powder metallurgy superalloys, Powder Metallurgy, 49 (**2006**) 2, 160–166

[4] J. S. Benjamin, Metallurgical Transactions, 1 (**1970**) 10, 2943–2951

[5] R. C. Reed, The Superalloys: Fundamentals and Applications, Cambridge University Press, United Kingdom 2006

[6] J. S. Benjamin, Mechanical alloying – A perspective, Metal Powder Report, 45 (**1990**) 2, 122–127

[7] M. J. Fleetwood, Mechanical alloying – The development of strong alloys, Material Science and Technology, 2 (**1986**) 12, 1176–1182

[8] P. Susila, D. Sturm, M. Heilmaier, B. S. Murty, V. Subramanya Sarma, Effect of yttria particle size on the microstructure and compression creep properties of nanostructured oxide dispersion strengthened ferritic (Fe-12Cr-2W-0.5Y_2O_3) alloy, Materials Science and Engineering A, 528 (**2011**) 13–14, 4579–4584

[9] Y. Estrin, S. Arndt, M. Heilmaier, Y. Brechet, Deformation behavior of particle-strengthened alloys: a Voronoi mesh approach, Acta Mater., 47 (**1999**) 2, 595–606

[10] M. P. Phaniraj, D. I. Kim, J. H. Shim, Y. W. Cho, Microstructure development in mechanically alloyed yttria dispersed austenitic steels, Acta Materialia, 57 (**2009**) 6, 1856–1864

[11] H. S. Kim, D. S. Suhr, G. H. Kim, D. W. Kum, Analysis of X-ray diffraction patterns from mechanically alloyed Al-Ti Powders, Metals and Materials, 2 (**1996**) 1, 15–21

[12] K. Zhang, I. V. Alexandrov, A. R. Kilmametov, R. Z. Valiev, K. Lu, The crystallite-size dependence of structural parameters in pure ultrafine-grained copper, J. Phys. D: Appl. Phys., 30 (**1997**) 21, 3008–3015

[13] L. Zhang, S. Ukai, T. Hoshino, S. Hayashi, X. Qu, Y_2O_3 evolution and dispersion refinement in Co-base ODS alloys, Acta Materialia, 57 (**2009**), 3671–3682

[14] C. Suryanarayana, M. Grant Norton, X-Ray Diffraction: A Practical Approach, Plenum Press, New York 1998

[15] S. Chen, Y. Zhou, Y. Li, S. He, Synthesis and characterization of Ni-Ti and Ni-Cr powders by mechanical alloying, J. Mater. Sci. Tech., 13 (**1997**), 86–90

[16] T. Chen, J. M. Hampikian, N. N. Thadhani, Synthesis and characterization of mechanically alloyed and shock-consolidated nanocrystalline NiAl intermetallic, Acta Materialia, 47 (**1999**) 8, 2567–2579

[17] J. Chihuaque, C. Patino-Carachure, J. O. Tellez-Vazquez, A. Torres-Islas, G. Rosas, Microstructural evaluation during mechanical alloying and air consolidation of Fe_3Al + (Li, Ni and C) intermetallic, Acta Microscopica, 19 (**2010**) 3, 305–311

[18] S. H. Chang, In situ TEM observation of γ', γ" and δ precipitations on Inconel 718 superalloy through HIP treatment, Journal of Alloys and Compounds, 486 (**2009**), 716–721

[19] G. Appa Rao, M. Srinivas, D. S. Sarma, Effect of thermomechanical working on the microstructure and mechanical properties of hot isostatically pressed superalloy Inconel 718, Materials Science and Engineering A, 383 (**2004**) 2, 201–212

[20] Md. Z. Alam, B. Srivathsa, S.V. Kamat, V. Jayaram, D. K. Das, Microtensile testing of a free-standing Pt-aluminide bond coat, Materials and Design, 32 (**2011**) 3, 1242–1252

[21] Schwarzkopf Plansee PM1000 Nickel alloy – Datasheet

[22] P. Jéhanno, M. Heilmaier, H. Kestler, M. Böning, A. Venskutonis, B. Bewlay, M. Jackson, Assessment of a powder metallurgical processing route for refractory metal silicide alloys, Metallurgical and Materials Transactions A, 36 (**2005**) 3, 515–523

[23] K. M. Youssef, R. O. Scattergood, K. L. Murty, C. C. Koch, Nanocrystalline Al-Mg alloy with ultrahigh strength and good ductility, Scripta Materialia, 54 (**2006**), 251–256

[24] M. Eskner, R. Sandstrom, Measurement of the ductile-to-brittle transition temperature in a nickel aluminide coating by a miniaturized disc bending test technique, Surface and Coatings Technology, 165 (**2003**), 71–80